

High-pressure instrument for small- and wide-angle x-ray scattering.

II. Time-resolved experiments

M. Steinhart^{a)}

*Institute of Macromolecular Chemistry, Academy of Sciences of the Czech Republic,
16206 Prague, Czech Republic*

M. Kriechbaum, K. Pressl, H. Amenitsch, and P. Laggner

Institute of Biophysics and X-Ray Structure Research, Austrian Academy of Sciences, 8010 Graz, Austria

S. Bernstorff

Sincrotrone Elettra, Basovizza, 34012 Trieste, Italy

(Received 29 May 1998; accepted for publication 17 September 1998)

An instrument to facilitate small- and wide-angle x-ray scattering measurements of samples under elevated hydrostatic pressures or exposed to pressure jumps is described. Pressure from atmospheric up to 0.35 GPa is produced by a motor-driven, piston-type generator and transferred through a network containing pressurizing liquid to a sample cell. The cell, with the optical path length of 1.6 mm, has two Beryllium windows with a total transmission of 0.4 (for x rays of $\lambda = 0.154$ nm) and low background scattering. Scattering can be observed at angles up to 30° . Samples can be solid or liquid with a minimal volume less than $30 \mu\text{l}$ and the irradiated volume up to $3 \mu\text{l}$. Separation of the samples from the pressurizing medium is accomplished by Teflon pistons. The high-pressure network has two sections separated by a pneumatic valve. The inner section is connected permanently to the cell and the outer one to the pressure generator. For pressure jumps, the outer section is brought to a different pressure level than the inner one and the jumps are accomplished by opening fast the connection between both sections. At the same time a trigger signal is sent to the data acquisition electronics. All functions of the instrument are PC controlled. To illustrate the performance characteristics of the instrument, time-resolved small-angle x-ray scattering measurements of phase transitions in liquid crystalline phospholipid, dioleoyl-phosphatidylethanolamine are shown. Pressure-jump experiments with 5 ms time resolution as well as temperature scans at a constant elevated pressure are presented. © 1999 American Institute of Physics. [S0034-6748(99)00102-1]

I. INTRODUCTION

High-pressure small-angle x-ray scattering (SAXS) alone or combined with wide-angle x-ray scattering (SWAXS) measurements on many biological and technological systems have recently attracted growing attention and several devices for this purpose have been built in various laboratories.¹⁻⁵ Understanding the dynamics of supra- and macromolecular processes is one of the objectives, which have stimulated the construction of high-flux synchrotron sources. The availability of these has been shifting the scope of interest to time-resolved measurements, of which processes induced by pressure jumps⁶⁻¹¹ are particularly important.

The advantages of pressure jumps over the more commonly used temperature jumps are mainly that they can be easily performed in both pressurizing and depressurizing directions, pressure changes are well defined, uniform within the sample volume, and fast in comparison with the time resolution of the measurement. This yields a potential to study the mechanisms of many processes, among the most important of which are mesomorphic phase transitions. This

potential makes it worthwhile to overcome principal difficulties and to construct high-pressure instruments.

SAXS and SWAXS techniques are commonly used to study the structure of complex systems, such as macromolecular solutions or liquid crystals. Their general properties and experimental requirements are quite special and complementary to methods, where high-pressure measurements are well established, e.g., spectroscopic or NMR¹² (see also Refs. in I). The pressures needed are not as extremely high as in solid state physics, where several hundreds of GPa can be achieved under laboratory conditions with the use of the diamond anvil cells.¹³ In the case of macromolecular dispersions, solutions, or crystals important changes take place under the pressures of the order of a few hundreds of MPa. The main task is, therefore, to optimize the instrument so that the excess scattering intensities are sufficiently high to accomplish a reasonable compromise between the quality of data and time resolution, which is, considering the present detector technology, on a millisecond scale. Generally, several microliters of sample are necessary. Technically, this means to make a compromise in many parameters, e.g., sample thickness versus irradiated volume, window thickness, and the accessible angle region. Reasonably low background scattering and low absorption are also important. An advan-

^{a)}Electronic mail: stein@imc.cas.cz

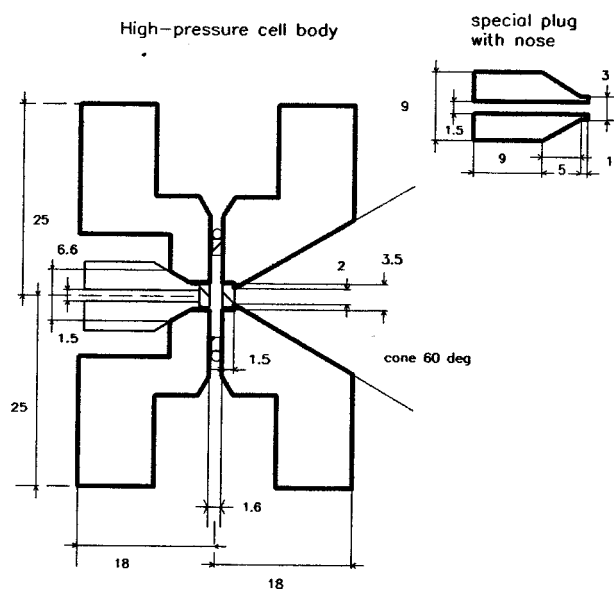


FIG. 1. Dimensions of the high-pressure cell in mm. The thickness is 22 mm. The plug, which supports the input Be window is depicted in the insert. Threads in the standard high-pressure connector holes $M 16 \times 1.5$ are not shown. Teflon pistons and drops of silicon oil are placed in the vertical bores.

tageous option in our case is the possibility to use the same cell both for static and time-resolved measurements so that successful experimental results can be obtained in laboratory conditions as well as at high-intensity synchrotron sources. The use of the latter facilities involves further requirements, which are not extremely important in a laboratory, such as a convenient, fast and reliable, remote control, quick assembly, disassembly and reproducible adjustment of the instrument, and its integration with the data acquisition electronics (DAQ).

The objective of this article is to describe the design and performance of a pressure-jump instrument suitable for SAXS and SWAXS, based on our existing system,¹⁴ optimized for time-resolved measurements. Representative results from our recent time-resolved measurements are also shown.

II. HIGH-PRESSURE X-RAY SAMPLE CELL (SAMPLE CELL)

A detailed drawing of the sample cell is depicted in Fig. 1. The cell was made by Nova Swiss (Nova Werke AG, Effretikon, Switzerland) according to our drawings of a special Cr-Ni-Mo-Ti steel. It is machined from a standard high-pressure cross piece and has three high-pressure connections. The first one, located in the optical axis, holds a plug, which supports the x-ray primary beam input window. This is a Be disk 1.5 mm thick, with a diameter of 3.5 mm of which 1.5 mm is unsupported. The x-ray scattering output window is of the same dimensions but it is permanently fixed (glued) to the sample cell body and its unsupported diameter is 2 mm. The total transmission of both windows is 0.40 for wavelength of 0.154 nm or 8 keV (see the Appendix). The

other two high-pressure connections are used to link the cell to the high-pressure network and to connect a thermocouple or a pressure sensor.

The optical path length (the sample thickness) is 1.6 mm. These dimensions correspond to a maximal irradiated volume of circa $3 \mu\text{l}$. By using plugs with different lengths of the nose, it is in principle possible to change the sample thickness up to a maximum of 2.5 mm.

The sample is separated from the pressurizing medium by cylindrical Teflon pistons, 3 mm long and 1.5 mm in diameter, placed in the bores perpendicular to the beam direction. Since these bores must also be partly filled with the sample, its optimal volume is circa 0.1 ml. In the case of samples where only small amounts are available as little as $30 \mu\text{l}$ can be used with proper care. On the other hand, if the sample is abundant, only the piston, separating the high-pressure network is necessary while the temperature sensor (or pressure sensor) can be fully immersed in the sample. This reduces the possibility of contamination of the sample. In spite of its simplicity, the separation by the pistons is good and our results indicate that typically more than 10 pressurizing and depressurizing cycles taking several hours can be performed before samples are measurably contaminated.

X-ray scattering can be measured from the small-angle region up to 30° . Intensities at angles up to 9° are not influenced by the effective-irradiated-sample-volume effect.¹⁴

Static measurements as well as pressure jumps can be made up to 0.35 GPa (3.5 kbar). An extension of this interval to 0.4 GPa is feasible; however, to meet a stringent safety factor, as demanded, e.g., by safety rules at synchrotron multiuser facilities, the pressure limit is 0.3 GPa.

The cell is horizontally sandwiched between two copper blocks, which are connected to a flow-through thermostat. During the whole series of measurements, the lower block is permanently fixed to the optical bench by means of a positioning table, from which it is thermally isolated by a Teflon spacer. The lower block is deepened by 2 mm so that the cell can be inserted reproducibly. To remove the cell, e.g., for changing a sample or cleaning, it is sufficient to unscrew only the upper block.

For measurements with a very accurate temperature control a special cell holder with Peltier elements and remotely operated control device has been designed.¹⁴

III. HIGH-PRESSURE NETWORK

For pressure jumps, the high-pressure network has two sections separated by a pneumatic valve (Nova Swiss). The outer section is connected permanently to the pressure generator, while the inner one is connected to the sample cell. The desired pressure is generated in the outer section and a pressure jump is accomplished by short cutting both sections. The main goals of the design were to minimize the number of parts, to make the total volume of the network as small as possible, and to make the volume of the inner section considerably smaller than that of the outer one. All the high-pressure parts, except the pneumatic valve are fixed to a portable Dural board of 10 mm thickness.

Details of the network are shown in Fig. 2. High pres-

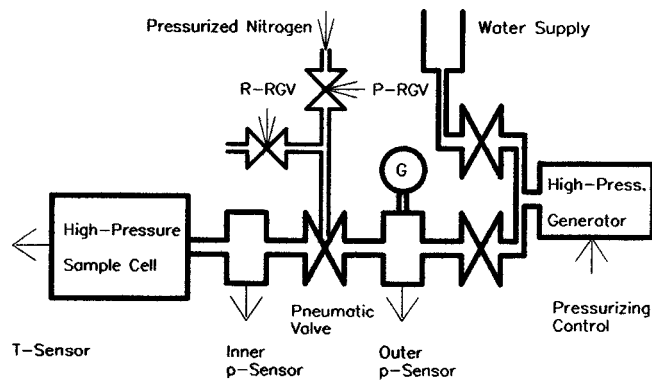


FIG. 2. Schematic drawing of the high-pressure network. P- and R-RGV are relay driven gas valves, which pressurize or release the pressure on the membrane of the pneumatic valve and thereby cause it to open or close. *G* is the Bourdon high-pressure gauge.

sure is generated by compressing pressurizing liquid with the use of the pressure generator (37-5.75-60, High Pressure Equipment Co. HIP, Erie, Pennsylvania, USA). This is in fact a very strong syringe rated for 0.41 GPa (60 000 PSI). It has 10 ml volume and 146 mm (5.75 in) travel of the shaft. It is operated by a three-phase motor ($0.37 \text{ kW}/1360 \text{ min}^{-1}$ or $0.55 \text{ kW}/1360 \text{ min}^{-1}$).

Water is used as the main pressurizing liquid. If the contact between the sample and water must be avoided, it is possible to separate water from the Teflon pistons by a drop of silicon oil.

The output of the pressure generator is connected to a double-stem valve. Its first connection separates the network from the pressurizing liquid reservoir. The second connection leads to a cross piece to which two pressure sensors are connected; a Bourdon gauge (HIP, USA) and an accurate pressure sensor (Sensotec, Columbus, Ohio, USA) with an electronic readout. The use of the former is not indispensable but for convenience and safety reasons the availability of pressure measurements, which are rough but always visible and independent of power sources and electrical connections, is highly recommended. The second pressure sensor is a fast and highly accurate pressure-to-voltage converter. Its readout and conversion of data into a serial RS232 signal is accomplished by a panel measuring instrument (Newport Electronics, USA). It has a single input with minimal sampling interval 100 ms and a high precision (six digits).

The last output of the cross piece is connected to the sample cell either directly, in the case of static measurements, or through a pneumatic valve. Nitrogen, pressurized to approximately 0.5 MPa, is employed and controlled by two relay-gas valves. The first one is used for pressurizing the membrane space of the pneumatic valve thereby opening the high-pressure connection. The second one is used to depressurize the membrane space, which leads to separation of the both sections of the high-pressure network.

For the long high-pressure connections (between the board, the pneumatic valve and the sample cell) a flexible high-pressure hose (NOVA SWISS 0.25 GPa) or preferably stainless steel high-pressure tubing can be used. The tubing must be carefully preshaped in such a way that even with its limited flexibility there is sufficient freedom for small move-

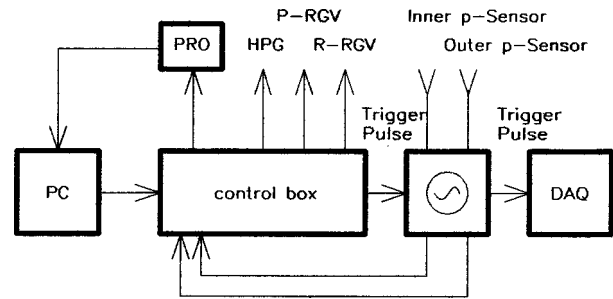


FIG. 3. Schematic drawing of the control and its integration into the measuring system. PRO is a pressure read-out device, in our case a panel multimeter, which displays the pressure, monitored by the selected pressure sensor, and converts it to a serial signal. Trigger pulses for the oscilloscope and data acquisition electronics are shown. HPG is the high-pressure generator.

ments of the cell (sometimes necessary for a fine adjustment) and the smallest possible tension builds up. The main advantages of the tubing are its smaller volume and higher pressure limit. In fact, not only is the high-pressure hose rated for lower pressure limit but mainly its relatively large volume (15 ml/m) would restrict the upper limit of pressure jumps to approximately 0.15 GPa, while the use of the pipe (2 ml/m) allows the full range up to 0.35 GPa. However, for static measurements the use of the hose is adequate.

A second pressure sensor is connected to the cell either directly or through a T piece in its near vicinity, in the case that an accurate temperature measurement requires a direct contact of the temperature sensor with the sample. When high-pressure tubing is used, the high-pressure network has a volume of circa 3 ml.

IV. MANUAL AND COMPUTER CONTROL

The control box is located close to all the components of the network, usually on the support board. It enables control of the main motor, which drives the pressure generator, the relay gas valves, switches between both pressure sensors and triggers the DAQ as is illustrated in Fig. 3.

Controlling of the main motor involves switching it on and off, safe changing of the direction of its rotation and sensing the end switch. At the present time, there is only one end switch, which functions in the depressurizing direction. It greatly increases the convenience and the safety of the system. A second end switch in the pressurizing direction would also be helpful but it is mechanically difficult to install it. Under normal conditions, excess movement in this direction is accompanied by an increase of pressure beyond a preset limit and therefore it is detected by at least one of the pressure sensors. Moreover, due to small volume of the network, the pressure of 0.35 GPa is reached at 1/4 of the piston path. This provides enough safety before the piston would reach the end and possibly damage the generator.

All main control functions can be performed manually using the switches on the control box. For remote control of both static and dynamic measurements two programs (in LabView language, National Instruments, USA) have been written. They enable manual-remote and automatic-remote control. Manual-remote control has advantages mainly in

simplicity of performing commands by a keyboard (or a mouse) while having an excellent overview of the network status. Moreover, the computer supervises some safety aspects such as proper succession of steps, e.g., when changing the direction of rotation of the motor or enforcing the pressure limits.

The automatic-remote control program enables reaching of any desired pressure automatically with high accuracy. During de- or pressurizing, pressure is periodically measured and the program estimates the time necessary to reach the final pressure taking into account the rate of current pressure change and the dead time of the device. The desired pressure can be reached with typical precision of 0.5% regardless of the amount of air in the network.

In the case of time-resolved measurements the pressure jump is started by a keystroke. The program sends a trigger pulse to the fast storage oscilloscope and through it to the DAQ and after a preset delay opens the pneumatic valve. The oscilloscope monitors the time dependence of pressure measured by both pressure sensors.

V. OPERATION

Cautious filling of the network with particular attention to remove air bubbles is essential.¹⁴ In the case of pressure jumps, trapped air bubbles affect the speed, with which the final pressure is reached and decrease its absolute value.

The best results are obtained when the network is filled with water during the assembly. First, the pressure generator is carefully filled by moving the piston several times up and down all the way. When a next component of the network is added, the piston moves forward until the component is fully filled. This procedure is repeated from the pressure generator to the point, where the cell is connected. The cell should be first substituted by a dummy piece (e.g., a T piece with two plugs) and the network should be tested at the highest required pressure. Then the cell must be filled with the sample and water (and optionally a drop of silicon oil) and connected to the network, preferably, while the pressure generator is running.

Pressure jumps are accomplished as follows:

- (1) The positioning of the cell on the optical bench is accomplished using an empty cell, not yet connected to the network.
- (2) If it does not contaminate the sample, the network including the cell should be tested for leakage by applying the maximum pressure presumed for the following experiment and then depressurized to the atmospheric pressure, preferably by a slowly opening the output to the water container.
- (3) After reaching the starting pressure in the inner section of the network, both sections are separated by closing the pneumatic valve.
- (4) A desired pressure must be established in the outer section. A simple preliminary calibration of the final versus original pressure will enhance the accuracy of the final pressure taking into account the finite volume of the inner section. If the network is without air bubbles and the volume of the inner section is relatively small the final

pressure is reached and stabilized in a few milliseconds. In the case of downward pressure jumps, care must be taken that the pressure in the network is never lower than atmospheric pressure. This can easily happen due to losses of the pressurizing liquid and it might result in unsealing of the windows since their support is not constructed to withstand large pressure difference in the opposite direction.

- (5) The DAQ as well as the oscilloscope monitoring pressure in both sections of the network must be started in a mode waiting for a trigger signal.
- (6) The pressure jump is started by remotely opening of the pneumatic valve. This valve instantly connects the inner and the outer sections, which leads to a quick pressure equilibration in the network. It is good practice to send the trigger pulse for the oscilloscope and DAQ slightly before the jump to obtain several frames of the static measurement of the initial (static) state.

The pressure generator could be disconnected during pressure jumps by the double-stem valve. However, its volume adds to the whole volume of the outer section so it is easier to reach the high final pressure, perhaps, at the expense of a little longer stabilization. The use of the double-stem valve mainly gives high flexibility in refilling the pressurizing medium while the inner section of the network may remain pressurized, etc.

In spite of small losses of the pressurizing medium the volume of the pressure generator is sufficient for running several pressurizing and depressurizing measurements without manual handling, which means also without entering the experimental hutch at the synchrotron radiation sources.

VI. PERFORMANCE OF THE INSTRUMENT

To demonstrate the performance (limits and resolutions) of the presented high pressure system we have investigated the barotropic and thermotropic phase transitions of a phospholipid/water dispersion using pressure jumps and temperature scans at constant elevated pressure. The static (equilibrium) p - T phase behavior of the phospholipid dioleoylphosphatidylethanolamine DOPE¹⁵ is already well characterized¹¹ and shows several well distinguishable structures, consisting of one-dimensional lamellar lattices (L_α, L_β) and a two-dimensional inverted-hexagonal (H_{II}) lattice within the p - T range accessible with our setup. By applying pressure-jumps and temperature-scans at different pressures, one can study the dynamics of these phase transitions when the system crosses the p - T phase boundary from one phase into another along the isothermic or isobaric line in the phase diagram.

Time-resolved x-ray diffraction experiments of pressure jumps were performed on the Austrian SAX-beamline 5.2 L at the synchrotron Elettra, Trieste, Italy.¹⁶⁻¹⁸

Figure 4 is a typical example of the signal output of the high-pressure sensor during a pressure jump (up and down) recorded by a storage oscilloscope. The slope during pressurizing is steeper (~ 0.1 GPa/5 ms) while depressurizing, where the pressure in the small volume of the cell is expanding into a much greater volume of the rest of the network, is

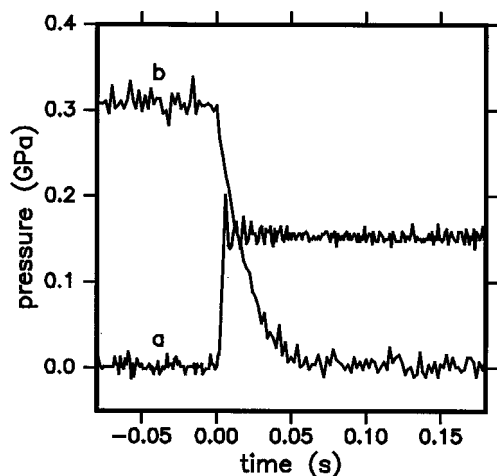


FIG. 4. A typical time dependence of the pressure in the sample cell during pressure jumps recorded by a 100 MHz digital storage oscilloscope. (a) p jump from atmospheric pressure to 0.15 GPa and (b) p jump between 0.31 GPa and the atmospheric pressure. The sharp spikes are caused by electronic noise.

considerably slower (~ 0.1 GPa/15 ms). During pressurizing from atmospheric pressure to 0.3 GPa, pressure is sufficiently stabilized within 30 ms whereas during depressurizing in the same pressure range within approximately 70 ms.

Figure 5 shows two examples of a time-resolved pressurizing and depressurizing jump of DOPE in excess water. The time-sliced diffraction patterns are presented in a contour plot, which illustrates clearly the evolution and disappearance of diffraction peaks in time before and after the initiation of the pressure jump. In both examples the first 50 frames have an exposure time of 5 ms with the pressure jump triggered at the 10th frame. These 5 ms frames are followed then by 180 frames of 50 ms and finally by 10 frames of 100 ms, summing up to a total time of approximately 10 s over which the relaxation of the system into the new equilibrium is recorded.

Depending on the response of the system to the jump and the signal/noise ratio the sequence of frames and their exposure times may be varied accordingly.

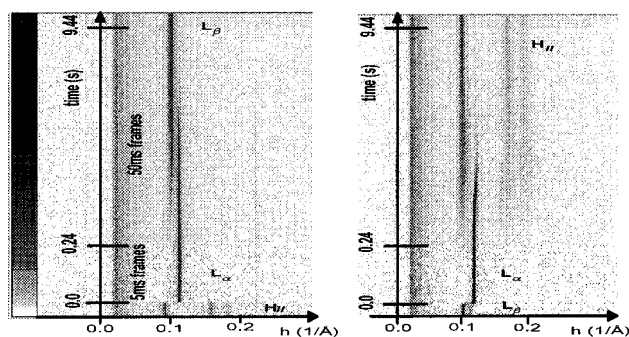


FIG. 5. Time-resolved SAXS patterns of barotropic phase transitions of DOPE initiated by pressure jumps. Each image consists of 256 time-sliced one-dimensional diffraction patterns in a two-dimensional reciprocal space vs time contour plot. (Intensity bar to the left) h is the magnitude of the scattering vector. The exposure time increases from initially 5 to 50 and 100 ms. The left part shows a pressurizing jump from 0.015 to 0.229 GPa at 20 °C. The right part shows a depressurizing jump from 0.25 GPa to the atmospheric pressure at 30 °C.

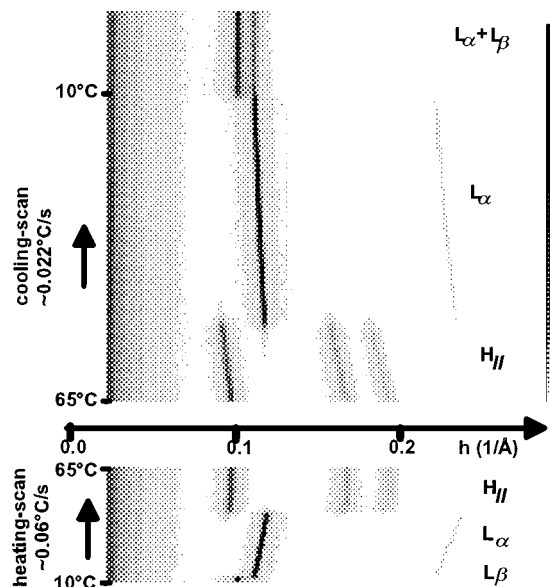


FIG. 6. Time-resolved SAXS patterns of thermotropic phase transitions of DOPE in a slow temperature scan at 0.123 GPa. The lower part shows heating and the upper one a cooling scan with scan rates depicted in the time axes. The exposure time is 10 s for each frame.

These measurements represent a particularly interesting case where the system undergoes two phase transitions during one pressure jump, i.e., starting from a pressure in the H_{II} region and jumping into the L_{β} phase and vice versa. In both cases the conversion has to pass the intermediate L_{α} phase. As can be seen from the time-resolved diffraction patterns, the final equilibrium phase is reached after about 8 s although the final equilibrium pressure is already reached within less than 50 ms after the jump. Immediately after such a “three-phase” jump (within the time resolution of our system) the structure converts into the intermediate L_{α} phase. After several hundreds of ms, the final L_{β} or H_{II} phases, respectively, begin to evolve, coexisting with the L_{α} phase for several seconds before it completely disappears. The duration of the coexistence after the jump is a function of the jump amplitude and temperature.

As a complementary study to these jump experiments slow temperature-scan studies of the same sample at elevated pressures are shown (Fig. 6). The setup is the same, except a larger sample-detector distance and the exposure times are 10 s frame. Alternatively also pressure scans at constant temperature (data not shown) are possible.

These experiments have clearly demonstrated the potential of time-resolved high-pressure SAXS/SWAXS experiments, which provide access to a new field of very interesting and important physicochemical phenomena.

VII. APPLICATIONS

A system for small- and wide-angle x-ray scattering under high hydrostatic pressure with a good cost/performance ratio was developed. Successful test measurements were performed using several SAXS cameras—a rotating anode source pinhole camera in our home lab, SAXS cameras on the synchrotrons DESY in Hamburg, Germany and Elettra, Trieste, Italy.

The large accessible angular range makes the cell well suited for scattering/diffraction measurements in the small- and wide-angle region on samples like solid polymers, liquid-crystalline probes, and biological model-membrane systems. Thus, information on the short- and long-range order can be obtained simultaneously, e.g., lattice and chain packing parameters in lyotropic lipid bilayers. Barotropic and thermotropic phase transitions of liquid crystalline systems at constant temperature or pressure, respectively, and their p - T phase diagram can be studied by using conventional x-ray sources and detectors or preferably high-flux synchrotron beam.

With sufficient primary-beam intensity, appropriate DAQ, and suitable samples the system is capable of time-resolved pressure-jumps experiments on the millisecond scale.

Of course, liquid crystalline samples, having sharp diffraction peaks well above the background in most of their phases, are very suitable for time-resolved measurements. Measurements of effects, which exhibit only weak diffuse small-angle scattering would involve problems with obtaining reasonably good statistics required for reliable data treatment.

APPENDIX: THE MEASUREMENT OF TRANSMISSION OF THE HIGH-PRESSURE SAMPLE CELL

A method using a strongly scattering standard sample measurement¹⁹ was modified to take into account the permanently changing intensity of the primary beam (due to stable decrease of the ring current) and use information from a desirable interval of channels.

In our modified method seven measurements were performed:

- (1) the standard sample and background,
- (2) the background,
- (3) the cell with one window, the standard sample and the background,
- (4) the cell with one window and the background,
- (5) the cell with two windows, the standard sample and the background,
- (6) the cell with two windows and the background, and
- (7) the standard sample and the background.

From the first and the last measurements the decrease with time of the primary beam was estimated using linear

approximation. Then all experimental intensities were corrected for this decrease. To calculate transmission we used twice the standard formula

$$T_x = \frac{(I_{xsb} - T_s I_{xb})}{(I_{sb} - T_s I_b)}.$$

Indices b , s , and x refer to the background, the standard sample (scatterer), and the measured sample, respectively.

The transmission of one (output) window is $T1 = 0.62$, the transmission of the cell with both windows is $T2 = 0.40$. These values are in a reasonable mutual agreement and also in accordance with the theoretical values.

ACKNOWLEDGMENTS

The authors are thankful for financial support from the Grant Agency of the Czech Republic (Grant No. 203/96/1387) and to the Academy of Sciences of the Czech Republic (Grant No. K2050602/12).

- ¹C. E. Kundrot and F. M. Richards, *J. Appl. Crystallogr.* **19**, 208 (1986).
- ²Yu. E. Gorbaty and A. V. Okhulkov, *Rev. Sci. Instrum.* **65**, 2195 (1994).
- ³C. Czeslik, R. Malessa, R. Winter, and G. Rapp, *Nucl. Instrum. Methods Phys. Res.* **368**, 847 (1996).
- ⁴P. T. C. So, S. M. Gruner, and E. Shyamsunder, *Rev. Sci. Instrum.* **63**, 1763 (1992).
- ⁵M. Lorenzen, C. Riekel, A. Eichler, and D. Häussermann, *J. Phys. IV* **3**, 487 (1993).
- ⁶J. Erbes, R. Winter, and G. Rapp, *Ber. Bunsenges. Phys. Chem.* **100**, 1713 (1996).
- ⁷M. Caffrey, J. Hogan, and A. Mencke, *Biophys. J.* **60**, 456 (1991).
- ⁸A. Mencke, A. Cheng, and M. Caffrey, *Rev. Sci. Instrum.* **64**, 383 (1993).
- ⁹A. Cheng, B. Hummel, A. Mencke, and M. Caffrey, *Biophys. J.* **67**, 293 (1994).
- ¹⁰A. Cheng and M. Caffrey, *J. Phys. Chem.* **100**, 5608 (1996).
- ¹¹F. Österberg, M. Kriechbaum, A. Polcyn, V. Skita, M. W. Tate, P. T. C. So, S. M. Gruner, and Sh. Erramili, *Phys. Rev. Lett.* **72**, 2967 (1994).
- ¹²J. Jonas and A. Jonas, *Annu. Rev. Biophys. Biomol. Struct.* **23**, 287 (1994).
- ¹³A. Ruoff, Xia Hui, Luo Huan, and Y. K. Vohra, *Rev. Sci. Instrum.* **61**, 3830 (1990).
- ¹⁴K. Pressl, M. Kriechbaum, M. Steinhart, and P. Laggnner, *Rev. Sci. Instrum.* **68**, 4588 (1997).
- ¹⁵P. T. C. So, Thesis, Princeton University, 1992.
- ¹⁶H. Amenitsch, S. Bernstorff, and P. Laggnner, *Rev. Sci. Instrum.* **66**, 1624 (1995).
- ¹⁷H. Mio, M. Chemloul, P. Laggnner, H. Amenitsch, S. Bernstorff, and M. Rappolt, *Nucl. Instrum. Methods Phys. Res. A* **392**, 384 (1997).
- ¹⁸H. Amenitsch, S. Bernstorff, M. Kriechbaum, D. Lombardo, H. Mio, M. Rappolt, and P. Laggnner, *J. Appl. Crystallogr.* **30**, 872 (1997).
- ¹⁹G. F. Neilson, *J. Appl. Crystallogr.* **6**, 386 (1973).